Eur. Phys. J. Appl. Phys. **45**, 20701 (2009)
DOI: 10.1051/epjap/2009005

THE EUROPEAN PHYSICAL JOURNAL APPLIED PHYSICS

Nucleation reduction strategy of $BaNH_4MgHPO_4$ (barium ammonium magnesium hydrogen phosphate, in vitro approach-1) crystals grown in silica gel medium and its characterization studies

P. Suresh[1], G. Kanchana[2], and P. Sundaramoorthi[1,a]

[1] Department of Physics, Thiruvalluvar Govt. Arts College, Rasipuram, 637401 Namakkal, India
[2] Department of Biochemistry, Muthayammal College of Arts and Science, Rasipuram, 637408 Namakkal, India

Received: 10 October 2008 / Received in final form: 20 November 2008 / Accepted: 4 December 2008
Published online: 31 January 2009 –

Abstract. Kidney stones consist of various organic, inorganic and semi-organic compounds. Mineral oxalate monohydrate and di-hydrate is the main inorganic constituent of kidney stones. However, the mechanisms for the formation of crystal mineral oxalate are not clearly understood. In this field of study there are many hypothesis including nucleation, crystal growth and or aggregation of formation of AOMH (ammonium oxalate monohydrate) and AODH (ammonium oxalate di-hydrate) crystals. The effect of some urinary species such as ammonium oxalates, calcium, citrate, proteins and trace mineral elements have been previously reported by the author. The kidney stone constituents are grown in the kidney environments, the sodium meta silica gel medium (SMS) provides the necessary growth simulation (in vitro). In the artificial urinary stone growth process, growth parameters within the different chemical environments are identified. The author has reported the growth of urinary crystals such as CHP, SHP, BHP and AHP. In the present study, $BaNH_4MgHPO_4$ (barium ammonium magnesium hydrogen phosphate) crystals have been grown in three different growth faces to attain the total nucleation reductions. As an extension of this research, many characterization studies have been carried out and the results are reported.

PACS. 34.50.Lf Chemical reactions – 33.20.Ea Infrared spectra – 87.55.N Radiation monitoring, control, and safety

1 Introduction

All kidney stones consist of a complex matrix with biominerals. The organic matrix has a composition that remains constant regardless of the type of crystals that make up the stone [1,2]. The urinary stone matrix accounts for approximately 3% of weight of a calculus [3]. From the analysis, the matrix compounds are soluble [4]. The most recent knowledge of the matrix has been described as a heterogeneous material composed of organic, inorganic and semi organic compounds like protein, lipids, carbohydrates and cellular minerals, etc. [5]. Proteins are the major constituents of stone matrices and the principle macromolecule in the urine [6]. Urinary proteins with the potential to adjust crystallization of mineral oxalates and calcium phosphate are Tamm-Horsfall protein, nephelomineralin, osteopontin, calprotectin, human serum albumin and urinary prothrombin fragment [5]. The kidney, chiefly by the renal tubular epithelial cells, produces most of the proteins. Other protein such as calprotectin, which is produced by granulocytes and commonly released at the sites of inflammation, has also been of concern in stone formation. The biominerals contain hard minerals like Ca, Ba, Sr, Mg and phosphates or its mixtures. The most common and important human body element of all the stones is calcium. Naturally calcium is found at concentrations of 8.9–10.1 mg/ml in the plasma [7]. Hypermineraluria is a biological syndrome defined as excretion in the urine of more than 0.1 mmol/kg/24 h of major minerals. Hypermineraluria is the most common metabolic abnormality in patients with nephrolithiasis [8]. Hypermineraluria raises urine supersaturation with respect to the solid phase of mineral complex with phosphate, enhancing the probability of self-nucleation and growth in to clinically significant stones. Urinary mineral excretion is continuously influenced by dietary intakes of calcium, sodium, protein, carbohydrates, alcohol, ammonium, trace element and potassium [9]. A mineral has been shown to bind to oxalate to form mineral oxalate monohydrate. Thus, mineral has been shown to affect the concentration of oxalate. In addition, oxalate is a major component of urinary stones

[a] e-mail: sundara78@rediffmail.com

and its urinary concentration plays an important role in stone formation. Even a small increase in urinary oxalate has a significant impact on mineral oxalate saturation. Although primary hyperoxaluria is relatively uncommon, patients with mineral oxalate stones have some degree of hyperoxaluria [10]. More amounts of oxalate can be obtained from foods such as nuts, chocolate, and dark green leafy vegetables [11]. A citrate concentration of plasma ranges from 0.05–0.03 mmoles/litre and it exits as an alkaline citrate [12]. Citrate inhibits crystallization of mineral oxalate and mineral phosphate by several mechanisms. (i) It decreases urinary saturation of mineral salts by complexion minerals and reducing ionic minerals concentration [13]. (ii) Citrate directly inhibits spontaneous precipitation of mineral oxalate [14], agglomeration of mineral oxalate [15], crystal growth of mineral phosphate [13] and heterogeneous nucleation of mineral oxalate by monosodium urate [16]. (iii) Citrate converts glycoproteins to an active disaggregated state probably by enhancing their inhibitor activity against the crystallization of calcium salts [17,18]. Due to the prohibitative role of citrate mentioned above, patients with hypocitraturia would be at a higher risk of minerals containing renal stones. This fact indicates that hypocitraturia is an important factor for stone formation.

The kinetic process of AOMH (ammonium oxalate monohydrate) nucleation and crystal growth requires super saturation [19], which can be obtained by excretion of the reactants in the urine (ammonium ion, calcium, trace elemental oxalate and water). A few molecules are combined together to form clusters. In the early step, clusters do not show a high degree of internal ordering. The longer time they exist, however, their degree of ordering increases by replacing internal salvation bonds by solid ion-ion bonds. Gradually, clusters become crystal embryos [20,21]. Above a critical size, embryos will grow into stable nuclei, and below some critical size, crystal embryos are too small and will reduce over all free energy by dissolving. The size of the nuclei is usually 100 Å or less [21]. Once a crystal nucleus has reached its critical size and super saturation ratio remains above one, the overall free energy is decreased by adding new crystal components to the nucleolus (self/spontaneous growth). This process is technically referred to as crystal growth.

2 Materials and methods

The silica gel also known as water glass was used in the present work as an intermediate growth medium. SMS (ARG-sodium meta silicate powder) was added to the double distilled water, in the ratio of 1:1, mixed, stirred well and kept undisturbed for few days to allow sedimentation. Then the clear top solution was filtered and stored in a light protected glass container. This is known as a stock solution [22]. Gel densities of 1.03–1.06 gm/cc were used. Simple test tubes of 25 mm diameter and 150 mm length were used as growth apparatus. The concentration of orthophosphoric acid used in this experiment was

Fig. 1. (Color online) Growth of $BaNH_4MgHPO_4$ crystals within the laboratory environment.

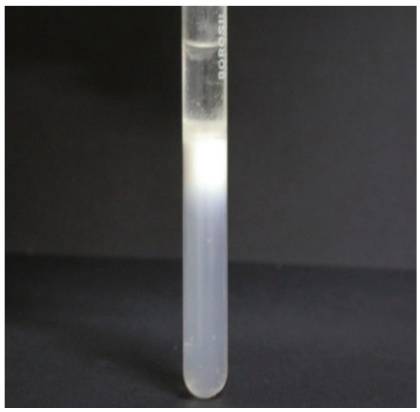

Fig. 2. (Color online) Growth of $BaNH_4MgHPO_4$ crystals within sunlight; exposed medium.

0.5N, 1N and 2N. The concentration of supernatant solution [$BaCl_2$+NH_4Cl_2+$MgCl_2$] varied from 0.5:0.5:0.5 M to 2:2:2 M [23,24]. One of the reactants orthophosphoric acid was mixed within the gel solution. The gel solution was taken as one third of its volume of the test tubes and after the gel set, the supernatant solution was added slowly along the sides of the test tubes. The mixture diffuses through the gel medium, which contains orthophorphoric acid and the self nucleation starts which in turn leads to the growth of $BaNH_4MgHPO_4$crystal.

The chemical reaction is:

$$Ba^{2+} + NH_4^{2+} + Mg^{2+} + HPO_4^{2-} + 2H_2O => BaNH_4MgHPO_4 \cdot 2H_2O + \text{Waste}.$$

The crystal growth processes were carried out in three different environments, one within laboratory environment, second one was sunlight exposed environment (day time only 7 h per day) and another one was continuous (with SMPS arrangement) semiconductor laser light exposed environment.

Table 1. Growth parameters of $BaNH_4MgHPO_4$ crystals (SDP).

SMS gel density gm/cc	Ortho phosphoric acid concentration in N	Gel+ H_3PO_4 pH value	Gel setting time in h	Supernatant solution concentration [barium chloride + ammonium chloride +$Mg(NO_3)_2 \cdot 2H_2O$] in M	Nucleation observed in hours	Growth period in days	Types of crystal observed
1.04	**2**	6.5	24	1:1:1	26	**170**	**Many poly crystals, Liesegang rings are observed**
		6.9	**10**	1:1:1	**20**		
		7.2	34	1:1:1	90		
	1	6.5	14	1:1:1	20	**180**	
		7.0	**1**	1:1:1	**60**		
		7.5	28	1:1:1	84		
1.05	**2**	**6.4**	**34**	1:1:1	**30**	**160**	
		6.9	**1**	1:1:1	**42**		
		7.3	48	1:1:1	68		
	1	6.5	16	1:1:1	23	**165**	**Single crystals**
		6.8	**1**	1:1:1	**40**		
		7.3	24	1:1:1	74		

N- Normality, M- Molarity.

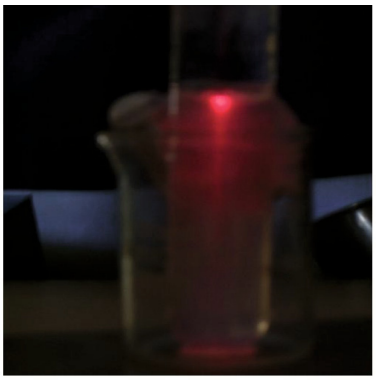

Fig. 3. (Color online) Growth of $BaNH_4MgHPO_4$crystals in laser light; exposed medium.

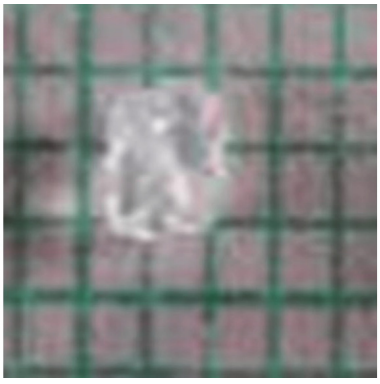

Fig. 4. (Color online) Harvested $BaNH_4MgHPO_4$ crystal.

3 Results and discussion

The $BaNH_4MgHPO_4$ crystals are grown in three different growth faces by applying various growth parameters. Figures 1–3 shows the growth of $BaNH_4MgHPO_4$ crystals at different growth environments and Figure 4 shows the harvested $BaNH_4MgHPO_4$ crystal. Table 1 gives the growth parameters of $BaNH_4MgHPO_4$ crystals and the bold letters shows the optimum growth parameters. Among them, the laser exposed (2 mW, 7300 Å of continues semiconductor laser light power and wave length are used) growth medium shows better nucleation reduction and no crystals were formed, because of the inability to attain super saturation. In sun light exposed medium partial nucleation was observed, since exposure of sunlight to the growth medium was only in the day time, that is eight hours per day and the growth period was six months.

Table 2. Comparative study of the FTIR-Spectrum of $BaNH_4MgHPO_4$ crystal.

S. No.	Bonds/vibrations	Reported values cm^{-1}	Observed values cm^{-1}	% of absorption value
01.	Ba, NH-Asymmetric stretching Mode& Hydrogen bond	3284	3271.69	1.165
02.	H-O-H Symmetric stretching bond	1651	1658.70	0.670
03.	NH in plane Stretching	1238.2	1237.71	0.680
04.	P=O bonding Stretching bond	1217–1137	1166.35	0.861
05.	PO_4 bond	1000–1100	1117.12	1.361
06.	PO_4-Asymmetric stretching mode	874	895.34	0.747
07.	Acid phosphate	577	565.27	0.810

3.1 FTIR spectral analysis of $BaNH_4MgHPO_4$ crystals

$BaNH_4MgHPO_4$-FTIR spectrum was recorded by using SHIMADZU FTIR-435 instrument. The FTIR spectrometer has KBr pellets sample holder and a KBr detector.

The KBr pellet samples were used and the absorption frequencies start in the range from 400 cm^{-1} to 4000 cm^{-1}. The spectrum was interpreted with the earlier reported values [25–27]. The absorption bonds, absorption frequencies and percentage of transmittance are tabulated in Table 2.

3.2 Thermo gravimetric (TGA and DTA) analysis of $BaNH_4MgHPO_4$ crystals

The TGA and DTA of $BaNH_4MgHPO_4$ crystals were carried out by STA 11500-PLTS instruments. The $BaNH_4MgHPO_4$ crystal, a 1.970 mg sample, was used for the TGA process. The TGA was ramped from room temperature to 750 °C by heating at a constant rate. The percentages of weight loss of the $BaNH_4MgHPO_4$ sample at a particular temperature are tabulated in Table 3.

The expected thermo-chemical reactions are:

$$BaNH_4MgHPO_4 \cdot 2H_2O \xrightarrow{\Delta} BaMgHPO_4 + NH_3 \uparrow + 2H_2O \uparrow$$

$$2BaMgHPO_4 \xrightarrow{\Delta} 2BaMg + (PO_4 \cdot H_2O) \uparrow + \frac{3}{2}O_2 \uparrow \text{ up to } 800\ ^\circ C.$$

Beyond 100 °C, the sample becomes anhydrous and after that it is hydrous along with ammonia up to 365 °C and 59% of the sample remained stable at the end of the analysis. Ba and Mg (barium, magnesium) are stable up to 750 °C.

3.3 Etching studies of $BaNH_4MgHPO_4$ crystal

A well-grown $BaNH_4MgHPO_4$crystal was immersed in HCl solution at a desired concentration. The dissolution of the $BaNH_4MgHPO_4$ crystal depends on the etchant concentration, temperature, crystal morphology, etching time, etc. Figure 5 shows the etch pits of $BaNH_4MgHPO_4$ crystal [28–31]. The etch pit patterns are observed as spirals, dendrites, vallies of ups, downs and straights.

3.4 Scanning electron microscopic studies of $BaNH_4MgHPO_4$ crystal

A well-grown $BaNH_4MgHPO_4$ single crystal was selected for the investigation of surface morphology of the grown crystal by using SEM. The SEM photograph was obtained in a version S-300-I instrument. The sample named as VCA-600 was kept in lobe middle; the data size was 640 × 480. The difference between the minor and major magnification of SEM was about 500 times. SEM acceleration voltage was 25 000 V and the sample was kept in high vacuum state. A 18 200-μm work distance was maintained and monochromatic color modes were employed. Figure 6 shows the SEM pattern of the $BaNH_4MgHPO_4$ crystal of 100 μm magnification [32–35].

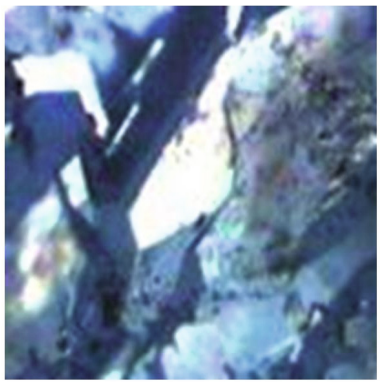

Fig. 5. (Color online) Etch pit pattern of $BaNH_4MgHPO_4$ crystal.

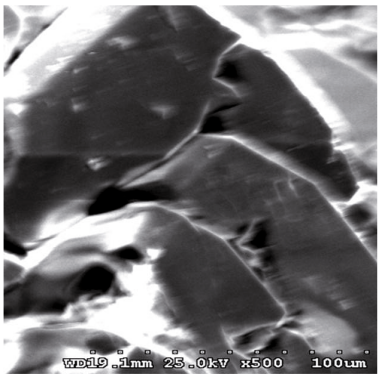

Fig. 6. SEM photo of a $BaNH_4MgHPO_4$ crystal.

3.5 X-ray diffraction

The XRD results revealed that the grown crystal was in single phase of $BaNH_4MgHPO_4$. The XRD pattern and diffraction indices of the grown crystals are calculated. Using the treor program crystal cell parameters are calculated. The unit cell parameters of $BaNH_4MgHPO_4$ crystals are $a = 8.0672$ Å, $b = 18.5739$ Å, $c = 22.7169$ Å and $\alpha = \beta = \gamma = 90°$. The crystal system is identified as *Orthorhombic*. The volume of the $BaNH_4MgHPO_4$ unit cell is 3403.88 $(Å)^3$.

4 Conclusion

The $BaNH_4MgHPO_4$ (barium ammonium magnesium hydrogen phosphate) crystals were grown at room temperature, and exposed to sunlight and laser medium. It was found that the $BaNH_4MgHPO_4$ crystal nucleation rate has been reduced more in the laser exposed medium than the sunlight-exposed medium, which is due to a variation of super saturations. The FTIR-spectrum recorded the functional group frequencies of $BaNH_4MgHPO_4$ crystal constituents. These results are recorded and compared with the reported values. Chemical etchings have been done at room temperature, which revealed the grown crystal defects. SEM analyses were also done and it reveals the

Table 3. TGA and DTA of $BaNH_4MgHPO_4$ crystal.

Points	TGA			DTA in °C
	Temperature (°C)	% of $BaNH_4MgHPO_4$ crystal present	Quantity of sample remaining in milligrams	
1	30	100	1.970	–
2	77.20	99.563	1.961	75.37
3	133.22	75.084	1.472	126.03
4	188.72	64.122	1.263	162.22
5	364.79	59.447	1.165	225.04
6	364.79	59.447	1.165	346.78
7	364.79	59.447	1.165	685.13
8	560	59	1.162	706.31
9	750	59	1.162	–

surface morphology of $BaNH_4MgHPO_4$ crystal. The decomposition temperature and percentage of weight loss of the grown crystal are recorded by TGA and DTA analysis. XRPD data provides the $BaNH_4MgHPO_4$ grown crystal cell parameters and its structure. This investigation results can be discussed with nephrologists and the results can be applied to the human physiological system in stepwise manner to avoid the renal stone formation. The crystal can be further investigated by atomic forced microscopy (AFM) to study the atomic orientation of renal stones with in the human physiological system.

References

1. S.R. Khan, P.O. Whalen, P.A. Glenton, J. Cryst. Growth **134**, 211 (1993)
2. W.H. Boyce, Am. J. Med. **45**, 673 (1968)
3. H.G. Tiselius, Clin. Chim. Acta **122**, 409 (1982)
4. R.W. Marshall, W.G. Robertson, Clin. Chim. Acta **72**, 253 (1976)
5. S.R. Khan, Urol. Int. **59**, 59 (1997)
6. R.L. Ryall, A.M.F. Stapleton, in *Calcium Oxalate in Biological System*, edited by S.R. Khan (CRC Press, 1995), pp. 45–62
7. C.G. Duarte, F.G. Knox, in *Text Book Of Renal Pathophysiology* (Harper and Row, 1978), pp. 82–90
8. F.L. Coe, J.H. Parks, J.R. Asplin, N. Engl. J. Med. **327**, 1141 (1992)
9. M. Audran, E. Legrand, Joint Bone Spine **67**, 509 (2000)
10. Y. Ogawa, T. miyazato, T. Hataano, World J. Surgery **24**, 1154 (2000)
11. D.S. Goldfarb, F.L. Coe, Am. Fam. Physician **60**, 2269 (2000)
12. D.P. Simpson, Am. J. Physiol. **224**, 223 (1983)
13. J.L. Mayer, L. Hsmith, Invest. Urol. **13**, 36 (1975)
14. M.J. Nicar, K. Hill, C.Y.C. Pack, J. Bone Miner. Res. **2**, 215 (1987)
15. D.J. Kok, S.E. Papapoulus, O.L.M. Bijvoet, Lancet **41**, 1056 (1986)
16. C.Y.C. Pak, Paterson, Arch. Intern. Med. **146**, 863 (1986)
17. B. Hess, Miner. Electrolyte Metab. **20**, 393 (1996)
18. C.Y.C. Pak, in *8th European symposium on Urolithiasis-Parma, Italy, June 9–12, 1999*, pp. 10–50
19. A. Mersmann, *Crystallization technology, Hand book*, 2nd edn. (Marcel Dekker, Inc., 2000)
20. V.A. Garten, R.B. Head, Phil. Mag. **14**, 1243 (1966)
21. D.J. Kok, *The Role Of Crystallization Process In Mineral Oxlates Urolithasis*, Ph.D. thesis, University of Leiden, 1991
22. H.K. Henisch, J. Electrochem. Soc. **112**, 627 (1965)
23. A.E. Alexander, P. Honson, *Colloid Science* (Clarendon Press, Oxford, 1949)
24. W. Eitel, in *Physical Chemistry of Silicate* (University of Chicago Press, 1954), pp. 60–95
25. Yean-Chin Dasai, J. Urol. **86**, 838 (1961)
26. C.M. Corns, Ann. Clin. Biochem. **20**, 20 (1983)
27. A. Hesse, D. Bach, *Stone analysis by IR spectroscopy, Clinical and laboratory Aspects*, edited by Alan Rose (University Park Press, Baltimore, 1982), pp. 87–105
28. J.J. Gilman, J. Johnsion, G.W. Sears, J. Appl. Phys. **29**, 749 (1958)
29. J.J. Gilman, J. Appl. Phys. **27**, 1018 (1956)
30. J.C. Fisher, in *Dissolutions and Mechanical Properties of Crystals* (John Wiley & Sons, New York, 1957), pp. 22-75
31. J.B. New Kirk, in *Director observation of Imperfection in crystals* (Interscience Publishers, New York, 1962)
32. K. Taukamot, J. Cryst. Growth **61**, 99 (1983)
33. H.C. Gates, in *Crystal growth and Characterization* (John Wiley & Sons, North Holland, 1975)
34. H. Bethage et al., *Electron Microscopy in Solid State Physics* (Elsevier, Amsterdam, 1987)
35. N. Albon et al., in *Growth and Perfection of Crystals* (Wiley, New York, 1958), p. 44